Supplement

S1. Discussion on the model improvements

The coke combustion in the ideal porous medium in Figure S1, where the coke deposition on the circle-like grains, was revisited to demonstrate improvements of the developed micro-continuum model compared to the previous LB models (Xu *et al.* 2018; Lei *et al.* 2021). The detailed initial condition, boundary condition, thermophysical properties and chemical kinetics can be found in the literature (Xu *et al.* 2018). The simulation results were analyzed to show the significance of the two-coupling between the chemical reaction and mass flow as well as the consecutive structural evolution due to the coke burning. Additionally, the computational performance between the LB model and the micro-continuum model was compared to present the advantage of the micro-continuum model in the simulation of the transient non-isothermal reactive flow.

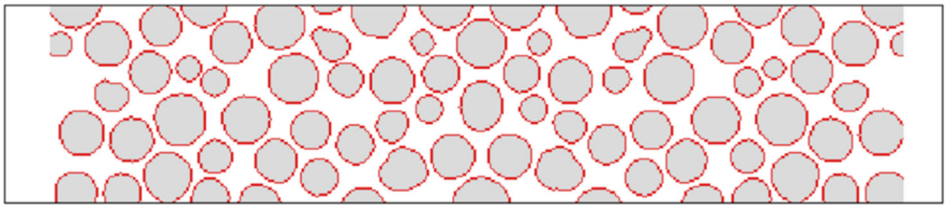

Figure S1: Representation of the ideal porous medium used for the previous study (Xu *et al.* 2018)

S1.1. Two-way coupling between the chemical reactions and mass flow

In the micro-continuum framework, the two-way coupling between the chemical reactions and mass flow was modelling to preserve the mass conservation in the reactive transport (Soulaine *et al.* 2017; Soulaine *et al.* 2018). Nonetheless, the assumption that the fluid flow was decoupled with the coke combustion reaction was made to simplify the computation of the mass flow in the previous studies using the LB models (Xu *et al.* 2018; Lei *et al.* 2021). With such an assumption, the gas continuity equation in the previous studies (Xu *et al.* 2018; Lei & Luo 2021) was given without the chemical source term, which neglected the effect of gaseous products on the mass flow. This assumption usually holds for those problems with slow chemical reaction rate and the single-phase liquid flow, such as mineral dissolution. However, the physical behavior of coke combustion with dramatic chemical reaction rates deviated from this assumption, leading to the significant underestimation of gas flow rate in Figure S2 and thus the combustion temperature in Figure S3. Detailly, this test case was simulated with the ignition temperature of 773 K and the average inlet velocity of 3.82×10^{-4} m/s. The relative error of the global mass conservation within the firing stage (t: 0~0.5 s) was measured, which was defined as the ratio of mass conservation error [mass accumulation - (mass flow in – mass flow out + mass production)] over the initial gas mass in the computational domain. The results show 0.0346% for the present model and -1840.1% for the previous model, indicating that the significant effect of gaseous products on the fluid mechanics cannot be neglected for the coke combustion. Figure

S2 illustrates contours of dimensionless velocity magnitude at the time instant t=2.91 s relative to the inlet velocity with/without the two-way coupling between the chemical reactions and the gas flow. The comparison demonstrated that the gas flow downstream the combustion front was accelerated by about two orders of magnitude since the gas production rate could reach $\mathcal{O}(10^{-5})$ kg/s, which was two orders of magnitude greater than the air injection rate of $\mathcal{O}(10^{-7})$ kg/s at the inlet. The accelerated gas fluid flow then enhanced the conjugate heat transfer between the gas and solid phases with the thermal-equilibrium combustion temperature decreasing by about 20 K, as indicated in Figure S3. Therefore, the burning temperature at the thermal equilibrium stage can be over-predicted regardless of the effect of the chemical source term on the non-isothermal reactive flow.

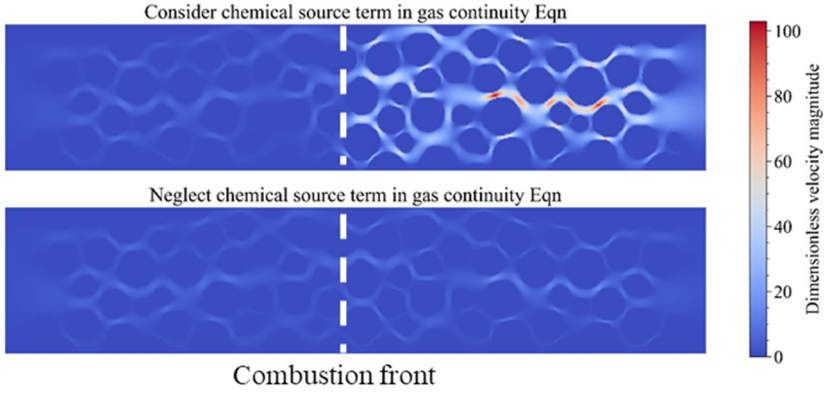

Figure S2: Revisited coke combustion problem for discussions on model improvements in the mass conservation: comparisons of simulated velocity magnitude contours at 2.91 s with/without considering chemical source term in the gas continuity equation. The combustion time of 2.91 s has reached the steady-state propagation of combustion front with the thermal equilibrium combustion

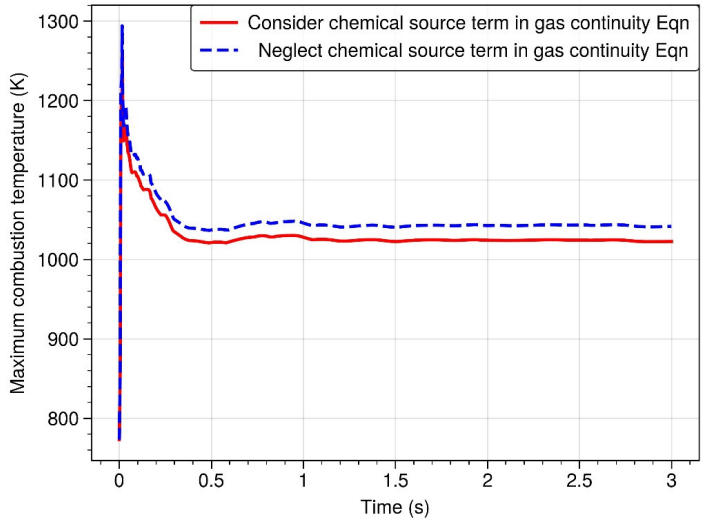

Figure S3: Revisited coke combustion problem for discussions on model improvements in the mass conservation: comparisons of the temporal evolution of maximum combustion temperature with/without considering chemical source term in the gas continuity equation

S1.2. *Energy conservation during structural evolution*

The numerical modeling of the coke combustion should account for the geometrical evolution with the phase change when the coke is exhausted. As illustrated in Figure S4, with the micro-continuum model, the temporal evolution of the coke volume fraction was continually tracked at each time step. As to the coupled energy conservation, the transient term of the energy balance equation considers the effect of the consecutive phase change on the energy balance. According to the sequential coupling strategy in Sect. 3.2 in the paper, the energy was rebalanced based on the updated coke volume fractions so that the released combustion heat was "timely" distributed to the fluid and solid phase with satisfying the conjugate heat transfer condition. As to the LB method, the volume of pixel (VOP) method was coupled to track the residual coke volume fraction, which evolved the coke cell into the fluid cell only when the residual coke is burned out, that is, the geometrical evolution of the coke phase became binary with the coke fraction being either zero or one. When solving the energy equation, the LB-VOP method with the binary geometrical evolution resulted in the unreliable energy balance due to the over-valued heat capacities without "timely" excluding volume fractions of the burn-out coke, and then slower combustion temperature rises than that predicted by the micro-continuum method with the continuous geometrical evolution. What is worse, the LB-VOP method needed to initialize the thermal distribution function of the computational node when the phase change took place with the same temperature as $T_{\mathrm{f},n+1}=T_{\mathrm{s},n}$ to ensure temperature continuity. This inappropriate treatment ignored the significant difference of the heat capacity between the gas phase and coke phase, which differed by two orders of magnitude, leading to the enthalpy discontinuity and vanished thermal energy during the geometrical evolution. For the revisited coke combustion problem with initial volume fractions of the rock and the coke being 0.498 and 0.0812, the disappeared thermal energy approximately occupied 10.0% ($\kappa=\dfrac{\rho_{\mathrm{coke}}c_{\mathrm{p,coke}}V_{\mathrm{coke}}}{\rho_{\mathrm{coke}}c_{\mathrm{p,coke}}V_{\mathrm{coke}}+\rho_{\mathrm{rock}}c_{\mathrm{p,rock}}V_{\mathrm{rock}}}$) in the total thermal energy of the solid phase. The gas temperature was then greatly under-predicted since most of the disappeared thermal energy should have been transported from the solid phase to the gas phase through conjugate heat transfer. Meanwhile, the relative error of the global energy conservation by the present model were calculated for the firing stage (t: 0~0.5 s), which was defined as the ratio of the energy conservation error [heat accumulation – (heat flow in + heat production – heat flow out – heat diffusion out)] over the initial total fluid and solid enthalpy in the computational domain. A very tiny relative error of 8.06×10^{-2}% justifies the excellent energy conservation by the present numerical model.

For better demonstration, temporal evolutions of the combustion temperature solved by the micro-continuum model and LB-VOP method are shown in Figure S5a, and the temperature contour at the time instant t=1.0 s are compared in Figure S5b as

well. At the start of combustion, the peak of combustion temperature for the case by the LB-VOP model was found to be 300 K lower than the case by the developed micro-continuum model. With the combustion developed into the steady stage, the temperature difference gradually dropped to about 50 K since the same thermal boundary conditions were imposed around the channel with the comparable thermal equilibrium condition. With such underestimation of the combustion intensity at the firing stage, the quantitative effect of operation parameters, including the ignition temperature and air flux, on the coke combustion phenomena might be incorrectly predicted with the LB-VOP method. Therefore, this study emphasizes the significance of continuous geometrical evolution modeling for the non-isothermal reactive flow by the developed micro-continuum method.

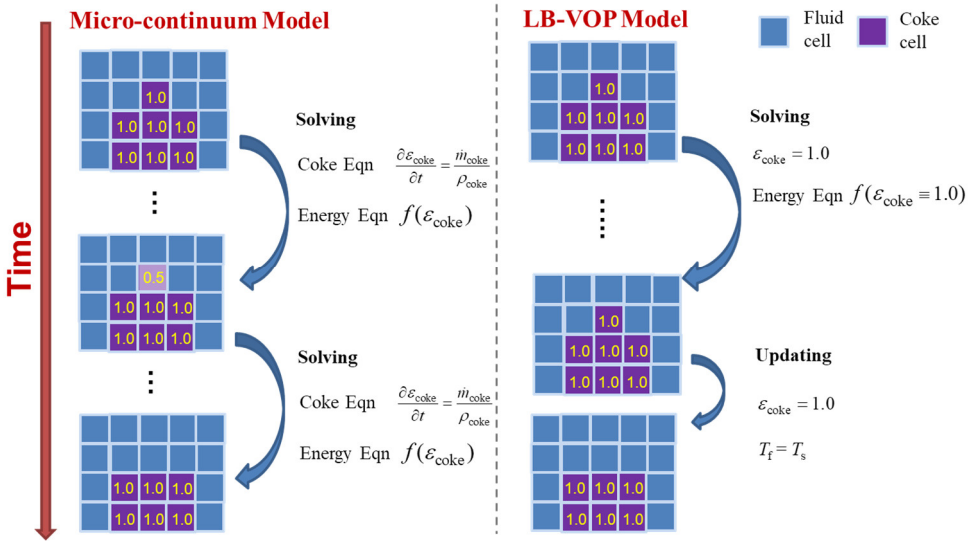

Figure S4: Schematic diagram of modeling approaches of the geometrical evolution and the energy balance with the continuous phase change by the micro-continuum model (left) and the binary phase change by the LB-VOP model (right) given that the protruding coke cell on the coke block is reacted and eventually turns to the fluid cell

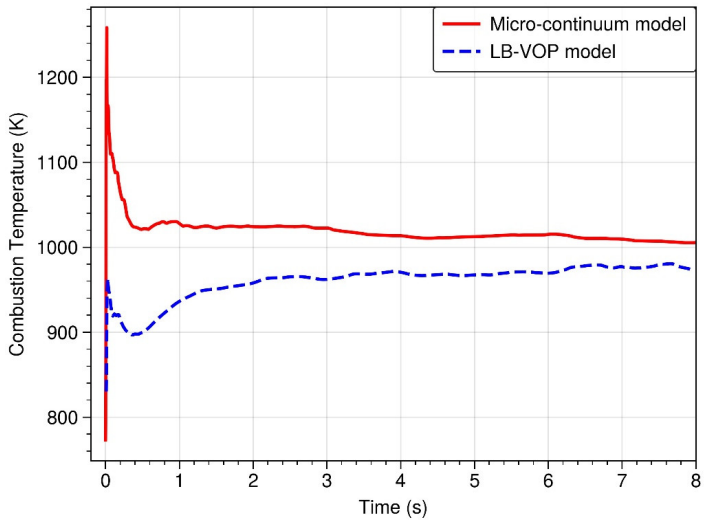

(a) Temporal evolution of combustion temperature

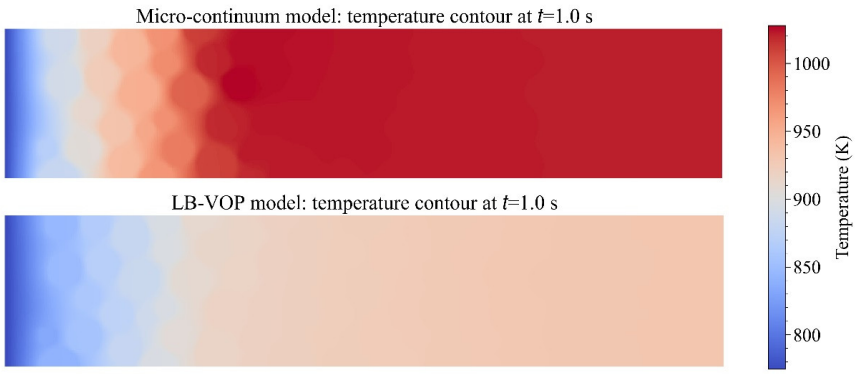

(b) Temperature contours at the time instant t=1.0 s

Figure S5: Revisited coke combustion problem for discussions on model improvements in the energy conservation: (a) comparisons of temporal evolutions of combustion temperature calculated by the micro-continuum model and LB-VOP model; (b) comparisons of the temperature contours at the time instant t=1.0 s calculated by the micro-continuum model and LB-VOP model

S1.3. *Computational performance of the micro-continuum model*

In opposite to the adjustable time step size by the present numerical implementation, the previous study using the single relaxation time (SRT) LB method fixed the time step to $\mathcal{O}(10^{-8})$ s due to the numerical stability constraint (Xu *et al.* 2018), which was three to five orders of magnitude lower than the present numerical method and thereby caused billions of time steps to accomplish the typical coke combustion with the physical duration of $\mathcal{O}(10)$ s. Despite the LB method exhibited excellent parallel scalability on the high-performance hardware, the small and fixed time step size of the SRT-LB method still significantly hindered the global computational efficiency in solving the unsteady nonlinear problem. The previous coke combustion problem (Xu *et al.* 2018) was simulated using the present micro-continuum model for the performance comparison. The computational duration dropped from about 200 h (SRT-LBM, 8 CPU) to about 6.5 h (Micro-continuum, 8 CPU) with about 30 times speedup in computational performance, indicating the outstanding performance of the micro-continuum framework in the area of unsteady non-isothermal reactive flow inside the complex porous medium. Owing to the increasing computational efficiency, the computational domain can be expanded from the $\mathcal{O}(10^5)$ meshes(Xu *et al.* 2018) to $\mathcal{O}(10^7)$ meshes, and the physical time duration can be extended from the $\mathcal{O}(1)$ seconds(Xu *et al.* 2018) to $\mathcal{O}(100)$ seconds for more physics, when one hundred of CPU cores are employed.

S2. Sensitivity analysis of the rock porosity ε_f on the simulation results

The sensitivity analysis of the rock porosity on the combustion dynamics and the numerical stability was performed for the ε_f values of 0.02, 0.01, 0.005 and 0.0025. With the decreasing rock porosity ε_f, the rock became much more impermeable, and the permeability got smaller, ranging from 1.57×10^{-5} mD to 8.33×10^{-3} mD. As shown Figure S6, the temperature profiles were almost identical when the rock porosity

was lower than 0.01. During the numerical tests, the extremely low porosity of $\varepsilon_f = 0.001$ and low permeability of $k = 10^{-9}$ mD were found to cause numerical instability under the high *Pe* condition, such as $Pe=10^{-2}$ and the average inlet velocity of 0.0021 m/s, since the great pressure drop within the rock region resulted in the divergence of the pressure computation. Therefore, the rock porosity $\varepsilon_f = 0.01$ was selected after considering the natural rock properties, the porosity-independence result and numerical stability.

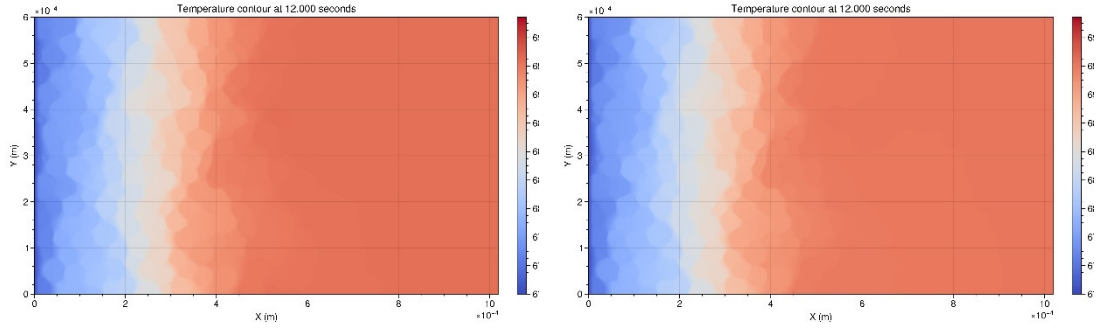

(a) $\varepsilon_f = 0.02,\ k = 8.33\times10^{-3}$ mD

(b) $\varepsilon_f = 0.01,\ k = 1.02\times10^{-3}$ mD

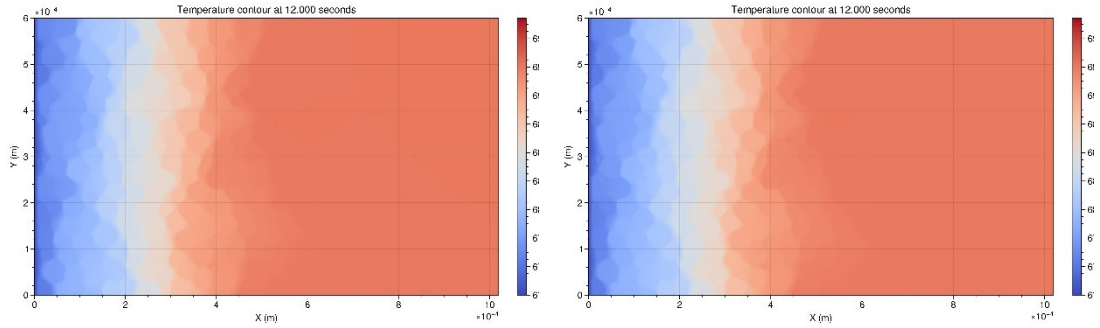

(c) $\varepsilon_f = 0.005,\ k = 1.26\times10^{-4}$ mD

(d) $\varepsilon_f = 0.0025,\ k = 1.57\times10^{-5}$ mD

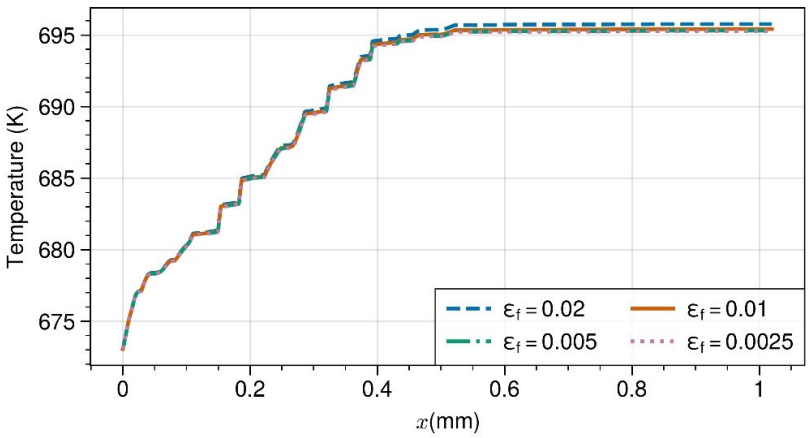

(e) temperature profiles at the channel mid-width

Figure S6: Comparisons of the temperature contours at *t*=12 seconds and the temperature profile at the mid-width of the channel among the rock porosity of 0.02, 0.01, 0.005 and 0.0025 ($Da_0 = 3.14\times10^{-3}$ and $Pe = 10^{-3}$).

129 REFERENCES

130 LEI, T. & LUO, K. H. 2021 Pore-scale simulation of miscible viscous fingering with dissolution
131 reaction in porous media. *Phys. Fluids* **33(**3**)**, 034134.
132 LEI, T., WANG, Z. & LUO, K. H. 2021 Study of pore-scale coke combustion in porous media
133 using lattice Boltzmann method. *Combust. Flame* **225**, 104-119.
134 SOULAINE, C., ROMAN, S., KOVSCEK, A. & TCHELEPI, H. A. 2017 Mineral dissolution and
135 wormholing from a pore-scale perspective. *J. Fluid Mech.* **827**, 457-483.
136 SOULAINE, C., ROMAN, S., KOVSCEK, A. & TCHELEPI, H. A. 2018 Pore-scale modelling of
137 multiphase reactive flow: application to mineral dissolution with production CO_2. *J.*
138 *Fluid Mech.* **855**, 616-645.
139 XU, Q., LONG, W., JIANG, H., ZAN, C., HUANG, J., CHEN, X. & SHI, L. 2018 Pore-scale
140 modelling of the coupled thermal and reactive flow at the combustion front during
141 crude oil in-situ combustion. *Chem. Eng. J.* **350**, 776-790.
142
143